Journal of Alloys and Compounds 489 (2010) L17–L21

Contents lists available at ScienceDirect

Journal of Alloys and Compounds

journal homepage: www.elsevier.com/locate/jallcom

Letter

Optical and photocatalytic properties of nanoparticulate $(TiO_2)_x(ZnO)_{1-x}$ powders

Aaron Dodd[a,*], Allan McKinley[b], Takuya Tsuzuki[c], Martin Saunders[d]

[a] Electron Microscope Unit, University of New South Wales, Kensington, New South Wales 2052, Australia
[b] School of Biomedical, Biomolecular and Chemical Sciences, The University of Western Australia, Crawley, Western Australia 6009, Australia
[c] Centre for Material and Fibre Innovation, Institute for Technology Research and Innovation, Deakin University, Geelong, Victoria 3217, Australia
[d] Centre for Microscopy, Characterisation and Analysis, The University of Western Australia, Crawley, Western Australia 6009, Australia

ARTICLE INFO

Article history:
Received 8 July 2009
Received in revised form
21 September 2009
Accepted 22 September 2009
Available online 1 October 2009

Keywords:
Oxide materials
Optical materials
Nanostructured materials
Mechanochemical processing
Optical properties

ABSTRACT

In this study, we have investigated the optical and photocatalytic properties of nanoparticulate $(TiO_2)_x(ZnO)_{1-x}$ powders that were synthesised by mechanochemical processing. The objective was to establish the suitability of these powders for use as optically transparent ultraviolet light screening agents. It was found that the photocatalytic activity of single phase ZnO can be substantially reduced through the incorporation of TiO_2 at the cost of a comparatively minor decrease in optical transparency. The composition given by $(TiO_2)_{0.10}(ZnO)_{0.90}$ was characterised by a photocatalytic activity that was approximately 20% of that exhibited by the ZnO powder synthesised using similar processing conditions. These results demonstrate that $(TiO_2)_x(ZnO)_{1-x}$ powders synthesised by mechanochemical processing are potentially useful as optically transparent ultraviolet light screening agents.

1. Introduction

Previous experimental studies have shown that mechanochemical processing can be used as a technologically simple and versatile method for manufacturing nanoparticulate powders of various semiconductor oxides, including ZnO [1,2], TiO_2 [3,4], and SnO_2 [5]. In this method, mechanically activated reaction of a salt precursor with an exchange reagent is used to synthesise a composite powder consisting of nanoparticulate grains dispersed within a salt matrix. Subsequent washing with a suitable solvent is then used to recover a nanoparticulate powder. This synthesis technique is of interest as it is capable of manufacturing high quality powders that are characterised by a controlled particle size and low levels of hard agglomeration [6].

Dispersions of semiconductor oxide nanoparticles find technological application as optically transparent ultraviolet (UV) light filters, such as protective paints and topical sunscreens. In such applications, semiconductor oxide nanoparticles are superior to chemical UV-absorbers in that they are chemically stable and are non-allergenic [7]. However, one issue of concern is heterogeneous photocatalysis. Absorption of UV-light results in the formation of electron–hole pairs, which can react with adsorbed surface species to generate highly reactive free radicals [8]. These free radicals can cause degradation of organic compounds present in the formulation [9]. In addition, it has been shown that photogenerated free radicals can damage DNA and RNA [10]. It is thus evident that an ideal nanoparticulate powder for UV screening applications would be characterised by low photocatalytic activity.

A wide variety of methods have been investigated as means of modifying the photocatalytic properties of nanoparticulate ZnO powders. Recently reported examples include doping with transition metal oxides [11,12], surface modification by coating with silica [13], and coupling with another semiconductor so as to alter the dynamics of charge carrier recombination [14].

In this study, mechanochemical processing has been used to manufacture nanoparticulate $(TiO_2)_x(ZnO)_{1-x}$ powders. The optical and photocatalytic properties of these powders were investigated with the objective of evaluating their suitability for use as optically transparent ultraviolet light screening agents.

2. Experimental details

2.1. Powder synthesis

Aqueous slurries of TiO_2 and ZnO were manufactured by a three-stage process consisting of mechanical milling, low temperature heat-treatment, and washing. In the first stage of processing, 10 g reactant mixtures were milled for 6 h within a hardened steel vial using a Spex 8000 mixer/mill. All millings used twenty 9.5 mm stainless steel balls as the grinding media. To ensure an inert atmosphere during milling, the grinding media and reactants were loaded into the vial whilst within a high-purity argon filled glovebox. The reactant mixtures that were used corresponded to those given by equations (1) and (2):

$$TiOSO_4 + Na_2CO_3 + 4NaCl \rightarrow TiO_2 + Na_2SO_4 + 4NaCl + CO_{2(g)} \quad (1)$$

* Corresponding author. Tel.: +61 2 9385 6709; fax: +61 2 9385 6400.
E-mail address: a.dodd@unsw.edu.au (A. Dodd).

0925-8388/$ – see front matter © 2009 Elsevier B.V. All rights reserved.
doi:10.1016/j.jallcom.2009.09.126

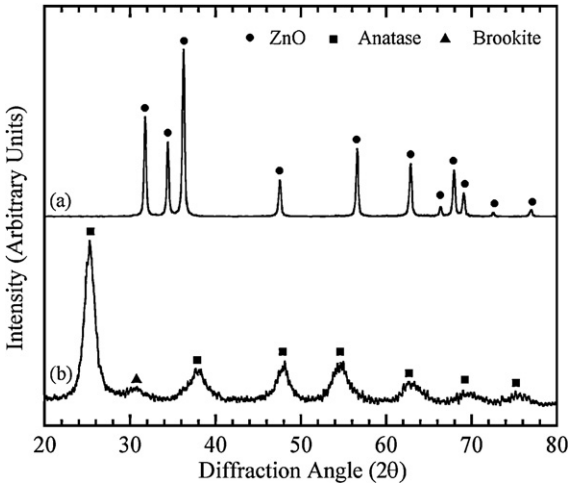

Fig. 1. XRD patterns of (a) ZnO and (b) TiO_2 powders.

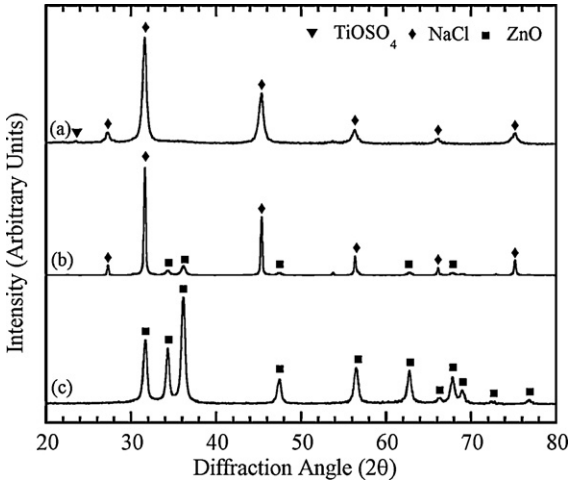

Fig. 3. XRD pattern of $0.1TiOSO_4 + 0.9ZnCl_2 + Na_2CO_3 + 4NaCl$ following: (a) milling for 6 h, (b) heat-treatment at 400 °C for 1 h, and (c) washing.

$$ZnCl_2 + Na_2CO_3 + 4NaCl \rightarrow ZnO + 6NaCl + CO_{2(g)} \quad (2)$$

Following milling, the reactant mixtures were heat-treated in air for 1 h at 400 °C. In the final stage of processing, the NaCl reaction by-product was removed by repeated washing with deionised water. Aqueous slurries of nanoparticulate $(TiO_2)_x(ZnO)_{1-x}$ were synthesised by the same overall method using the ZnO synthesis system for which a given amount of $ZnCl_2$ was substituted with a molar equivalent of $TiOSO_4$.

All of the reactant mixtures employed in this study contained NaCl diluent. The primary purpose of the NaCl diluent was to improve the milling characteristics of the reactant powder charge. In the absence of any NaCl diluent, the reactant mixtures became caked onto the interior of the milling vial, which prevented effective processing of the precursors. The secondary purpose of the NaCl diluent was to lower the volume fraction of the oxide particles in the salt by-product so as to promote the formation of dispersed single-crystal particles [6].

Washed slurries were divided into two portions. The first portion of slurry was dried so as to allow analysis of the powder particles by X-ray diffraction and BET gas adsorption. The second portion was used in the undried state to prepare samples for transmission electron microscopy, UV–vis spectroscopy, and photocatalytic testing.

2.2. Characterisation techniques

The chemical evolution of the reactant mixtures during processing was followed by X-ray diffraction (XRD) using a Siemens D5000 diffractometer with Cu Kα radiation. The average crystallite size of the washed powders was estimated from the full-width half-maximum breadth of the diffraction peaks using the Scherrer equation [15].

The specific surface area of the washed and dried powders was measured by five-point BET gas adsorption using a Micromeritics Tristar instrument. All powders were vacuum degassed at 150 °C for 1 h prior to analysis.

A Cary 2E UV–visible spectrophotometer was used to measure the absorption spectra of the washed slurries. The spectra were measured over the wavelength range of 200–800 nm with an optical path length of 10 mm. Samples were prepared by diluting the washed slurries down to 0.01 wt.% with Milli-Q water. Dispex N400 was added 10 wt.% relative to the solids content. Prior to measurement, the diluted suspensions were subjected to intense ultrasonication for 15 min.

The particle size and morphology of the washed powders were examined by transmission electron microscopy (TEM) using a JEOL 2000FX microscope. Elemental distribution maps of the washed $(TiO_2)_{0.1}(ZnO)_{0.9}$ were derived using energy filtered imaging with a JEOL 3000F microscope equipped with a Gatan image filter. Samples for TEM were prepared by ultrasonically dispersing a small quantity of the aqueous slurry in a 0.10 wt.% solution of stearic acid in hexane and then evaporating a drop of the dispersion on a carbon coated specimen grid.

2.3. Photocatalytic testing

Samples for photocatalytic testing were prepared by diluting the washed slurries down to a solids content of 0.02 wt.% with Milli-Q water. Following dilution, the slurries were subjected to intense ultrasonication for 15 min in order to disperse the particles within the suspension. Immediately prior to measurement of the photocatalytic activity, 1 mL of a 30 mM solution of 5,5-dimethyl-1-pyrroline-N-oxide (DMPO) spin-trap was added to 10 mL of the powder suspension.

The photocatalytic activity of the washed powders was characterised by measuring the hydroxyl radical concentration following irradiation with UV-light using the spin-trapping technique with electron paramagnetic resonance (EPR) spectroscopy [16–18]. Samples were irradiated for 100 s with 300 nm light from a 1 kW Hg–Xe lamp whilst within a quartz flat cell that was located in the cavity of the EPR spectrometer. A monochromator was attached to the lamp to select the irradiation wavelength. The relative concentration of photogenerated hydroxyl radicals was measured by recording the intensity of the first central line of the first derivative EPR spectrum corresponding to the DMPO-OH spin adduct.

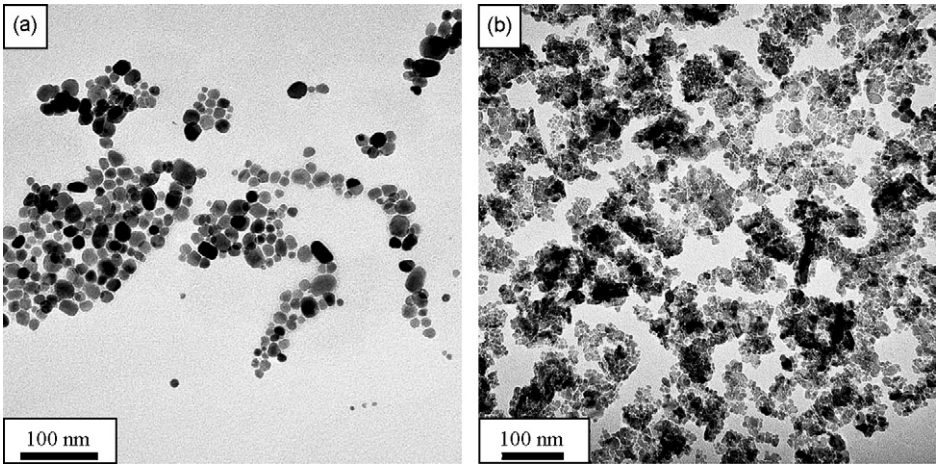

Fig. 2. Bright field TEM images of (a) ZnO and (b) TiO_2 powders.

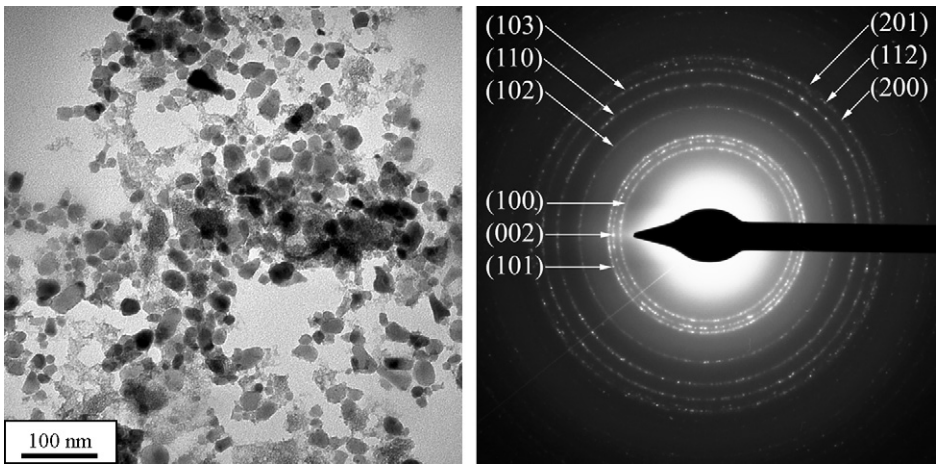

Fig. 4. Bright field TEM image of the washed $(TiO_2)_{0.1}(ZnO)_{0.9}$ powder and its corresponding selected area diffraction pattern.

3. Results and discussion

3.1. Synthesis of ZnO and TiO_2

Powders of ZnO and TiO_2 were synthesised for the purpose of providing baseline comparisons for the optical and photocatalytic properties of the $(TiO_2)_x(ZnO)_{1-x}$ powders. The reaction systems that were used to synthesise these ZnO and TiO_2 powders have previously been reported in the literature [1–3]. Similar results were obtained in this study. In particular, both powders were found to be crystalline and were characterised by a nanoscale crystallite size. This is illustrated in Fig. 1, which shows XRD patterns of the washed ZnO and TiO_2 powders. The pattern of the ZnO powder corresponds to the expected wurtzite structure with a crystallite size of approximately 17 nm. The pattern of the TiO_2 powder shows that it consists predominantly of anatase with a small proportion of brookite. Analysis of the diffraction peak breadth gave a crystallite size of approximately 6 nm for the major anatase constituent.

Fig. 2 shows bright field TEM images of (a) ZnO and (b) TiO_2 powders that were synthesised by mechanochemical processing. The ZnO powder consists predominantly of dispersed nanoparticles with a reasonably narrow particle size distribution. In contrast, the TiO_2 powder consists of small crystallites that are strongly agglomerated into large secondary aggregates. For both powders, the observed primary particle size is consistent with the crystallite size determined from the XRD peak broadening.

3.2. Synthesis of $(TiO_2)_x(ZnO)_{1-x}$

The $(TiO_2)_x(ZnO)_{1-x}$ powders were prepared using the basic ZnO synthesis system for which a given amount of the $ZnCl_2$ reactant was substituted with a molar equivalent of $TiOSO_4$. All of the reactant mixtures for the synthesis of $(TiO_2)_x(ZnO)_{1-x}$ were found to exhibit similar behaviour during processing irrespective of the doping level. As a representative example, Fig. 3 shows the XRD pattern of the $0.1TiOSO_4 + 0.9ZnCl_2 + Na_2CO_3 + 4NaCl$ reactant mixture following (a) milling for 6 h, (b) heat-treatment at 400 °C for 1 h, and (c) washing. The pattern of the as-milled powder consists solely of broadened diffraction peaks corresponding to NaCl and $TiOSO_4$. Heat-treatment resulted in sharpening of the NaCl peaks and replacement of the $TiOSO_4$ peak with those corresponding to ZnO. Following washing, only the ZnO peaks remained, indicating the successful removal of the salt matrix. Analysis of the diffraction peak breadth showed that the crystallite size of the ZnO component was effectively unchanged by incorporation of $TiOSO_4$ into the reactant mixture.

The only peaks visible in the XRD pattern of the as-milled powder were those of NaCl and $TiOSO_4$. This is consistent with previous experimental studies regarding the synthesis of ZnO and TiO_2 nanoparticles by mechanochemical processing [1–3]. Tsuzuki and McCormick found that $ZnCl_2$ reacts with Na_2CO_3 during milling to form poorly crystalline $ZnCO_3$ [1]. $TiOSO_4$ has been shown to only react with Na_2CO_3 during post-milling heat treatment [3].

No peaks corresponding to any TiO_2 phase were evident in the diffraction pattern of the washed $(TiO_2)_x(ZnO)_{1-x}$ powders. It would thus appear that the TiO_2 reaction product was incorporated into an amorphous oxide phase. Supporting evidence for this conclusion is provided by bright field and energy filtered TEM imaging. Fig. 4 shows a bright field TEM image of the washed $(TiO_2)_{0.10}(ZnO)_{0.90}$ powder and its corresponding selected area diffraction pattern. Two clearly distinct particle morphologies are evident in the bright field image. All of the rings in the diffraction

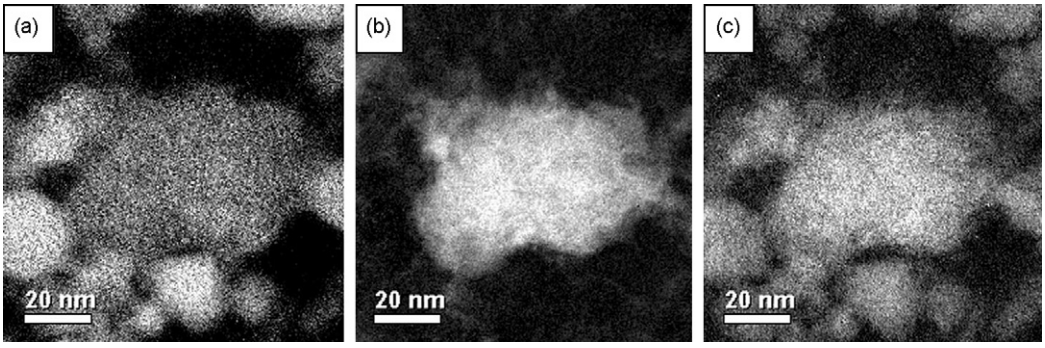

Fig. 5. Energy filtered TEM images of $(TiO_2)_{0.1}(ZnO)_{0.9}$ showing the distribution of (a) zinc, (b) titanium, and (c) oxygen.

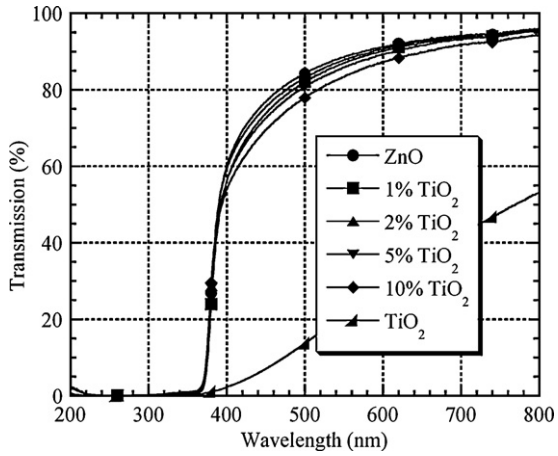

Fig. 6. Transmission as a function of wavelength for aqueous suspensions of the ZnO, $(TiO_2)_x(ZnO)_{1-x}$, and TiO_2 powders.

pattern can be indexed to the wurtzite structure of ZnO. Energy filtered imaging, shown in Fig. 5, reveals that the powder consists of ZnO particles and a mixed oxide phase that contains both zinc and titanium.

Formation of an amorphous zinc–titanium oxide by solid-state reaction of ZnO with TiO_2 has previously been observed by Ocana et al. [19]. In their study, an amorphous TiO_2 layer was deposited on preformed ZnO particles by the hydrolysis and condensation of titanium butoxide in an ethanolic solution. Subsequent calcination at 700 °C resulted in solid-state chemical reaction between the ZnO and the TiO_2 to form an amorphous zinc titanate.

3.3. Optical properties

Fig. 6 shows transmission as a function of wavelength for aqueous suspensions of the ZnO, TiO_2, and $(TiO_2)_x(ZnO)_{1-x}$ powders. All of the suspensions exhibited strong attenuation of UV-light as a consequence of band-gap absorption. In the optical wavelength region, the single phase ZnO suspension was the most transparent due to its fine particle size and high degree of dispersion [1,2]. The TiO_2 powder was also characterised by a small crystallite size. However, the optical transparency of the TiO_2 suspension was significantly lower due primarily to the heavily agglomerated state of the dispersion [3]. All of the $(TiO_2)_x(ZnO)_{1-x}$ dispersions were characterised by an optical transparency that was only marginally less than that of the single phase ZnO.

3.4. Photocatalytic activity

Fig. 7 shows the specific surface area and DMPO-OH yield of the ZnO, TiO_2, and $(TiO_2)_x(ZnO)_{1-x}$ powders. It can be seen from this figure that the single phase ZnO powder was characterised by the highest photocatalytic activity of all the compositions studied despite having the lowest specific surface area. The TiO_2 powder possessed the highest specific surface area but gave a DMPO-OH yield that was only 76.8% that of the single phase ZnO powder. These results are consistent with previous experimental studies regarding the relative activity of ZnO and TiO_2 [20–22]. For example, Wang et al. investigated the activity of various oxide semiconductors for the photocatalytic degradation of methyl orange [20]. The TiO_2 sample used in their study was found to be less than half as active as the ZnO despite having a significantly greater specific surface area.

The photocatalytic activity of the $(TiO_2)_x(ZnO)_{1-x}$ powders decreased monotonically with the TiO_2 content. This is attributable to an increased amount of the amorphous mixed oxide phase present in the powder. An amorphous, or at least poorly crystalline,

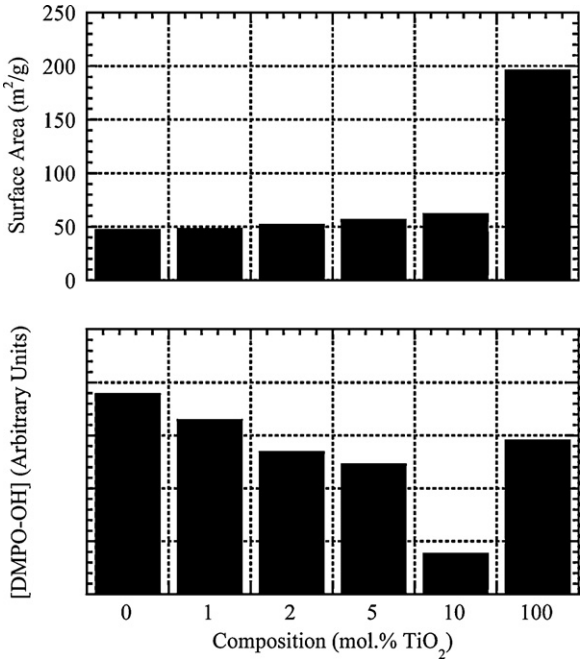

Fig. 7. Specific surface area and DMPO-OH yield for the ZnO, $(TiO_2)_x(ZnO)_{1-x}$, and TiO_2 powders. The DMPO-OH yield is shown in arbitrary units.

phase would be expected to exhibit low photocatalytic activity due to the high concentration of crystal imperfections, which are able to act as efficient recombination centers for photogenerated charge carriers [23–25]. Similar results have been obtained by Ohtani et al. [25] in a study of the photocatalytic activity of TiO_2 powders that were prepared by heat treatment of an amorphous precursor. Using various probe reactions, it was demonstrated that the photocatalytic activity of amorphous TiO_2 is negligible and that the activity increases nearly linearly with the proportion of crystalline anatase present in the powder.

4. Conclusions

In this study, solid-state chemical reaction of anhydrous salt precursors with Na_2CO_3 in the presence of NaCl diluent has been used to manufacture nanoparticulate powders of ZnO, TiO_2, and $(TiO_2)_x(ZnO)_{1-x}$. The photocatalytic activity of these powders was characterised by measuring hydroxyl radical yield following exposure to UV-light using the spin-trapping technique with electron paramagnetic resonance spectroscopy. It was found that the single phase ZnO powder was characterised by the highest level of photocatalytic activity. The $(TiO_2)_x(ZnO)_{1-x}$ powders were significantly less photoactive and their dispersions were characterised by a slight reduction in optical transparency. This combination of low photocatalytic activity and reasonably high optical transparency indicates that these powders are potentially useful as optically transparent ultraviolet light screening agents.

References

[1] T. Tsuzuki, P. McCormick, Scripta Mater. 44 (2001) 1731.
[2] A. Dodd, A. McKinley, M. Saunders, T. Tsuzuki, J. Nanopart. Res. 8 (2006) 43.
[3] A. Dodd, A. McKinley, T. Tsuzuki, M. Saunders, J. Phys. Chem. Solids 68 (2007) 2341.
[4] P. Billik, G. Plesch, Mater. Lett. 61 (2007) 1183.
[5] L. Cukrov, T. Tsuzuki, P. McCormick, Scripta Mater. 44 (2001) 1787.
[6] P. McCormick, T. Tsuzuki, J. Robinson, J. Ding, Adv. Mater. 13 (2001) 1008.
[7] N. Serpone, D. Dondi, A. Albini, Inorg. Chim. Acta 360 (2007) 794.
[8] M. Hoffman, S. Martin, W. Choi, D. Bahnemann, Chem. Rev. 95 (1995) 69.
[9] A. Ricci, M. Chrétien, L. Maretti, J. Scaiano, Photochem. Photobiol. Sci. 2 (2003) 487.

[10] H. Hinode, S. Horikoshi, N. Serpone, J. Knowland, J. Photochem. Photobiol. A 111 (1997) 205.
[11] A. Dodd, A. McKinley, T. Tsuzuki, M. Saunders, Mater. Chem. Phys. 114 (2009) 382.
[12] Q. Xiao, L. Quyang, J. Alloys Compd. 479 (2009) L4.
[13] J. Wang, T. Tsuzuki, L. Sun, X. Wang, J. Am. Chem. Soc. 92 (2009) 2083.
[14] S. Janitabar-Darzi, A. Mahjoub, J. Alloys Compd. (2009), doi:10.1016/j.jalcom.2009.07.071.
[15] B. Cullity, Elements of X-ray Diffraction, 2nd ed., Addison-Wesley, Reading, 1978.
[16] C. Jaeger, J. Phys. Chem. 83 (1979) 3146.
[17] E. Janzen, Acc. Chem. Res. 4 (1971) 31.
[18] M. Grela, M. Coronel, A. Colussi, J. Phys. Chem. 100 (1996) 16940.
[19] M. Ocana, W. Hsu, E. Matijevic, Langmuir 7 (1991) 2911.
[20] C. Wang, B. Xu, X. Wang, J. Zhao, J. Solid State Chem. 178 (2005) 3500.
[21] N. Serpone, P. Maruthamuthu, P. Pichat, E. Pelizzetti, H. Hidaka, J. Photochem. Photobiol. A 85 (1995) 247.
[22] S. Kansal, M. Singh, D. Sud, J. Hazard. Mater. 153 (2008) 412.
[23] O. Carp, C. Huisman, A. Reller, Prog. Solid State Chem. 32 (2004) 33.
[24] K. Eufinger, D. Poelman, R. Gryse, G. Martin, Appl. Surf. Sci. 254 (2007) 148.
[25] B. Ohtani, Y. Ogawa, S. Nishimoto, J. Phys. Chem. B 101 (1997) 3746.